

Shape Coexistence in ^{78}Ni and the new Island of Inversion centred in ^{74}Cr

F. Nowacki,^{1,2} A. Poves,³ E. Caurier,^{1,2} and B. Bounthong^{1,2}

¹Université de Strasbourg, IPHC, 23 rue du Loess 67037 Strasbourg, France

²CNRS, UMR7178, 67037 Strasbourg, France

³Departamento de Física Teórica e IFT-UAM/CSIC,
Universidad Autónoma de Madrid, E-28049 Madrid, Spain
and Institute for Advanced Study, Université de Strasbourg

(Dated: December 9, 2024)

Large Scale Shell Model calculations (SM-CI) predict that the region of deformation which comprises the heaviest Chromium and Iron isotopes at and beyond $N=40$ will merge with a new one at $N=50$ in an astonishing parallel to the $N=20$ and $N=28$ case in the Neon and Magnesium isotopes. We propose a valence space including the full pf -shell for the protons and the full sdg shell for the neutrons; which represents a come-back of the the harmonic oscillator shells in the very neutron rich regime. The onset of deformation is understood in the framework of the algebraic SU(3)-like structures linked to quadrupole dominance. Our calculations preserve the doubly magic nature of the ground state of ^{78}Ni , which, however, exhibits a well deformed prolate band at low excitation energy, providing a striking example of shape coexistence far from stability.

PACS numbers: 21.60.Cs, 21.10.-k, 21.10.Re

Introduction. The origin of the chemical elements around us and the limits of nuclear stability are among some of the actual burning questions in nuclear physics. The answers to these fundamental questions challenges our theoretical understanding and description of nuclei. In addition, the link between nuclear structure in neutron-rich systems and nucleosynthesis has been established for long now, and for example modeling the composition of neutron-star crusts depends strongly on binding energies and structure of nuclides near $N=50$ and $N=82$ shell closures [1]. The experimental exploration of regions of very neutron rich nuclei has recently unveiled the details of the shape coexistence in ^{68}Ni and the existence of a new region of deformation (or Island of Inversion, IoI) surrounding ^{64}Cr [4–13]. Large scale shell model calculations predicted first, and later explained in detail, this behavior [14, 15], in particular for the strong similarity of the mechanisms driving deformation and collapse of shell closures at $N=40$ and $N=20$. Another recent experimental and theoretical finding is the merging of the IoI's at $N=20$ and $N=28$ [16, 17]. One of the popular recent mechanism responsible for the shell evolution and collapse of spin-orbit shell closures far from stability was introduced by Tokyo group [2] and could be due to the tensor force. Although this mechanism is supported experimentally in light systems such as in ^{42}Si at $N=28$, the strong shell closure ^{132}Sn at $N=82$ contradicts it and the question remains open in ^{78}Ni at $N=50$. In addition, in view of these precedents, we asked ourselves if an equivalent phenomenon of IoI merging might occur for $N=40$ and $N=50$, and this question prompted this study whose results support fully the conjecture. In the meantime, there has been new experimental measures on the Chromium and Iron isotopes up to $N=42$ and $N=46$ respectively, which seem to support it as well [18], and

interesting theoretical explorations of the physics close to ^{78}Ni [19], which will help us a lot in the present investigation.

Valence space and effective interaction. In our previous studies of the physics around ^{68}Ni we proposed a valence space with a ^{48}Ca core, comprising the full pf -shell for the protons and the orbits $1p_{3/2}$, $1p_{1/2}$, $0f_{5/2}$, $0g_{7/2}$, and $1d_{5/2}$ for the neutrons. Ideally one should have included the neutron orbit $2s_{1/2}$ to complete the Quasi-SU(3) multiplet which is dominant in the region [20], but at the time this was beyond our computing possibilities, and we thought that its absence would not harm severely our model, as indeed it was the case. Why should intruder configurations produce shape coexistence in ^{78}Ni and deformed ground states in ^{76}Fe and ^{74}Cr ? The answer, as expected, resides in the interplay of the spherical mean field and the quadrupole-quadrupole correlations. Therefore, we should ensure that the chosen valence space can incorporate them properly. In addition, we would like to preserve a certain (even if imperfect) continuity among the different valence spaces that we have used in this broad mass region. For $N=Z$ up to ^{100}Sn these have been discussed in detail in reference [20]. In particular, the shell model interpretation of the superallowed decay of doubly magic $^{100}\text{Sn} \rightarrow ^{100}\text{In}$ ($\log ft=2.4$) was made in the full sdg -shell for neutrons and protons [21]. In fact, even if we do not put it at use in this article, we aim to define an interaction covering all the $pf - sdg$ potential valence spaces. For the protons, the natural space up to $Z=32-34$ is indeed the full pf shell, which will bring in quadrupole collectivity of Quasi or Pseudo-SU(3) type [22, 23] depending on the number of protons and the value of the $Z=28$ gap. In the neutron side, as we add neutrons in excess of $N=40$, the role of the neutron pf -shell orbits is slowly transferred to the companion orbits

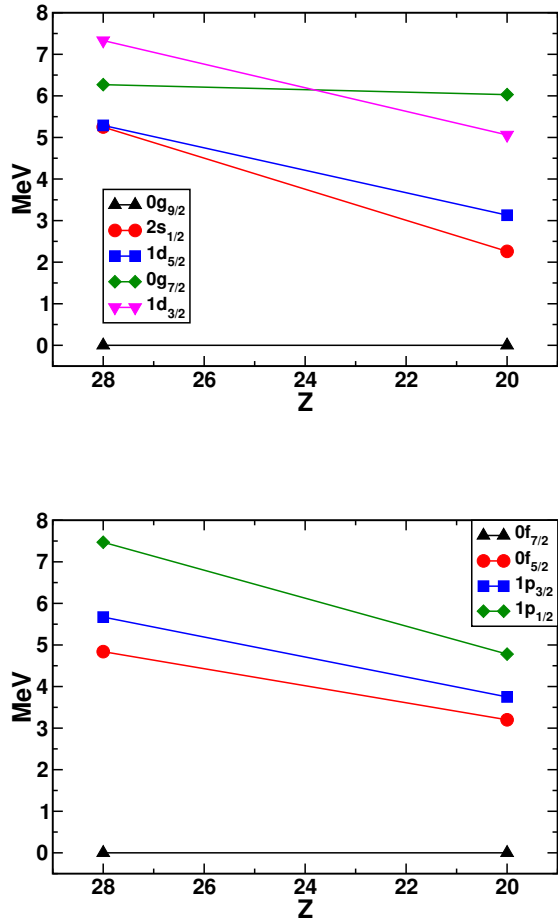


FIG. 1. (color online). Neutron gaps at N=50 (upper panel). Proton (Z=28) gaps at N=50 (lower panel).

of the $0g_{9/2}$ in the sdg major oscillator shell. Unfortunately, size prevents us to following the transition from N=40 to N=50 keeping both sets of neutron orbits in our valence space, but we expect a smooth transit from one space to another. In the N=40 valence space, the neutron collectivity is provided by the Pseudo-SU(3) coherence of the holes below N=40 and the Quasi-SU(3) coherence of the particles above it. And the mean field regulator is the N=40 gap. Close to N=50 the build up of collectivity is different. Particles above N=50 should develop Pseudo-SU(3) coherence, whereas holes in the $0g_{9/2}$ will help with their single shell quadrupole strength. The mean field regulator is now the N=50 gap. In brief, the valence space in this article comprises the p=3 harmonic oscillator (HO) shell (pf) for the protons and the p=4 HO shell (sdg) for the neutrons.

Our starting effective interaction matrix elements are based on the free nucleon-nucleon interaction of reference [24], regularised and renormalised with the G-matrix

techniques of reference [25]. We modify their monopole part in order to reproduce the experimental evolution of the regulating gaps in the model space, drawing on the experience acquired in our previous work in the adjacent regions. The final choice leads to the values of the gaps gathered in Figure 1. We name the resulting interaction PFS DG-U. The dimensions of the matrices to be diagonalised are at the edge of present computer capabilities for solving the problem exactly, in several cases reaching 10^{10} M=0 Slater determinants.

The Quasi+Pseudo SU(3) heuristics. We Follow in this section our paper on N=Z nuclei [20]. The goal is to locate the most favourable configurations from the point of view of an schematic monopole plus quadrupole-quadrupole hamiltonian, in the limit of maximal quadrupole dominance. For the N=50 isotones the protons which are in the Quasi-SU3 space ($0f_{7/2}$, $1p_{3/2}$) contribute the following values to the intrinsic mass quadrupole moment (bare masses are used): $Q_0^m(\pi)=11.5, 12.5, 14.0, 9.4$ and 0 b², for Z=28, 26, 24, 22, and 20 respectively. The neutron $0p-0h$ configurations have zero quadrupole moment. For the $2p-2h$ configurations the two neutrons are in the Pseudo-SU3 space ($0g_{7/2}$, $1d_{5/2}$, $1d_{3/2}$, $2s_{1/2}$). Their contribution to $Q_0^m(\nu)$ is 14.7 b². The two neutron holes in $0g_{9/2}$ add 8 b². For the $4p-4h$ neutron configuration the values are 22.2 b² and 10.7 b², respectively (b is the HO length parameter). The total intrinsic quadrupole moments that we should use to compute the mass deformation parameter do need effective "masses" which we take equal to the standard isoscalar charge ($q_\pi(1.31)+q_\nu(0.46)=1.77$). Doing so we get typical values $\beta_m=0.24$ for the $2p-2h$ configurations and $\beta_m=0.30$ for the $4p-4h$ ones. Let's now compute the energies of the np-nh configurations using the following expression adapted from ref. [20]:

$$E_n = G_n^{mp}(50) - \hbar\omega\kappa \left(\frac{\langle Q_0^m(\pi) \rangle}{15 b^2} + \frac{\langle Q_0^m(\nu) \rangle}{23 b^2} \right)^2 \quad (1)$$

with $\hbar\omega\kappa=3.0$ MeV. $G_n^{mp}(50)$ contains the monopole gaps plus a pairing correction:

$$G_n^{mp}(50) = n \left(\frac{3.0}{8} n_f^\pi + 2.25 \right) + \Delta(n) + \delta_p(n) \quad (2)$$

The term $\Delta(n)$ takes into account the quadratic monopole contribution to the np-nh configurations which amounts to -0.9 and -4.4 MeV for the $2p-2h$ and $4p-4h$ cases, and $\delta_p(n)$ gives an estimation of the extra pairing energy of the np-nh configurations (-1 MeV and -2 MeV for n=2 and n=4).

In Figure 2 we have plotted the quadrupole energies of the np-nh configurations from equation 1 for the five isotones of interest. We have checked these results via direct diagonalization of the quadrupole-quadrupole interaction

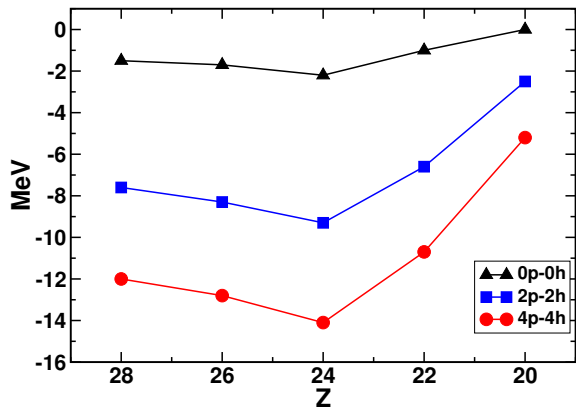


FIG. 2. (color online). Quadrupole energies of the np-nh configurations in the N=50 isotones.

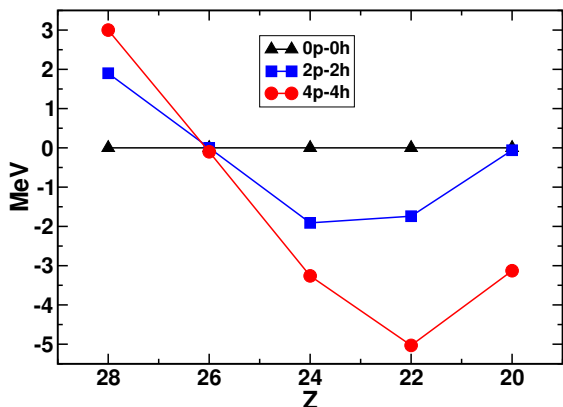


FIG. 3. (color online). Relative position of the bandheads of the np-nh configurations predicted by our schematic model (see text).

with the same strength than in equation 1 and the agreement with the analytic expression proposed in ref. [20] is excellent. Once the gaps calculated with equation 2 are plugged in equation 1 we obtain the relative position of the np-nh band heads in the isotopes of interest, that we gather in Figure 3. In ^{78}Ni the 0p-0h configuration, the N=50 closed shell, is the lowest with both 2p-2h and 4p-4h deformed states appearing at low energy. It is seen also in the figure that very rapidly the deformed 4p-4h band becomes yrast in ^{74}Cr , and ^{72}Ti and remains so even in ^{70}Ca . Notice that whereas the maximum gain of quadrupole energy of the 4p-4h deformed configuration takes place in ^{74}Cr , the maximum total energy gain oc-

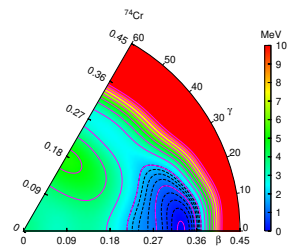
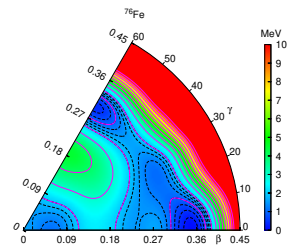
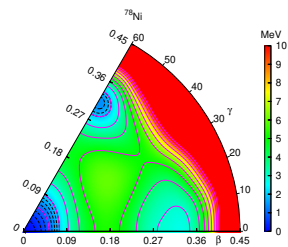


FIG. 4. (color online). Potential Energy Surfaces for ^{78}Ni , ^{76}Fe , and ^{74}Cr with the interaction PFSGD-U.

urs at ^{72}Ti , due to its smaller neutron gap. Therefore, the quasi-pseudo SU3 approach suggests a doubly magic ground state in ^{78}Ni with coexisting low-lying deformed bands and deformed yrast bands of (mainly) 4p-4h nature in the remaining isotopes.

Potential Energy Surfaces. In order to better grasp the meaning of the exact results in the intrinsic frame we have performed Angular Momentum Projected Hartree Fock calculations in the SM valence space using the PFSGD-U interaction. The results are displayed as contour plots in the (mass) β - γ plane (aka Potential Energy Surfaces PES) in Figure 4. It is seen that at the mean field level, ^{78}Ni is a spherical doubly magic nucleus in its ground state with deformed oblate and prolate minima nearby. ^{76}Fe has instead two minima, one prolate and another oblate connected by the γ degree of freedom. In the case of ^{74}Cr , the landscape is fully dominated by the prolate solution. These deformed structures have typically $\beta \sim 0.3$.

Spectroscopic results. Let's move now to the predictions of the full fledged diagonalizations using the inter-

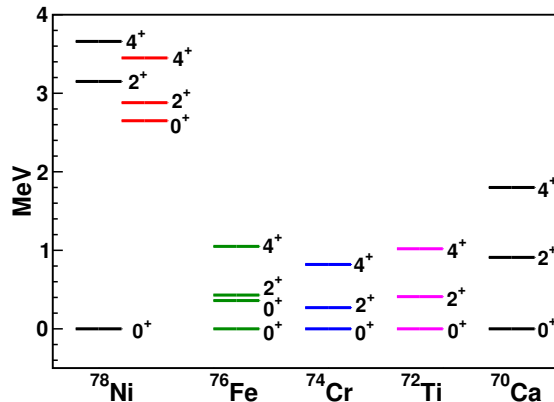


FIG. 5. (color online). Theoretical spectra of the N=50 isotones with the PFS DG-U interaction.

TABLE I. E2 properties of the yrast states of the N=50 isotopes. Energies in MeV, B(E2)'s in $e^2\text{fm}^4$, Q_s 's in efm^2 .

	B(E2)				Q_s	
	E_{2^+}	E_{4^+}	$2^+ \rightarrow 0^+$	$4^+ \rightarrow 2^+$	2^+	4^+
^{78}Ni	2.88	3.45	32	783	-39	-65
^{76}Fe	0.43	1.05	314	707	-45	-57
^{74}Cr	0.27	0.82	536	781	-47	-61
^{72}Ti	0.41	1.02	321	506	-34	-45
^{70}Ca	0.91	1.80	119	194	-3	+8

action PFS DG-U, starting with the results at fixed number of neutron excitations across the N=50 closure. For this calculations we do not impose any truncation in the proton sector. The goal of this exercise is to check the resilience of our Quasi+Pseudo SU3 collective structures to the presence of a sizeable proton gap and non degenerated Pseudo-SU3 neutron orbits. The structure of the 2p-2h and 4p-4h bands are very similar for all the isotopes (except ^{70}Ca) although the relative position of the three bandheads is indeed different and close to the values of Figure 3. In ^{74}Cr , their energies (4p-4h, 0.0 MeV, 2p-2h, 1.4 MeV and 0p-0h, 2.4 MeV) are in fair quantitative agreement with the predictions of our schematic model. In addition, the 2p-2h and 4p-4h configurations correspond to well deformed rotors with a nearly perfect $J(J+1)$ spacing and B(E2)'s consistent with deformation parameters very close to the ones obtained in the SU3 limit (we use standard effective charges $q_\pi=1.31$ and $q_\nu=0.46$). All in all, a very satisfactory result. For the 2p-2h yrast band of ^{74}Cr we have $E(2^+)=0.27$ MeV and $B(E2)(2_1^+ \rightarrow 0_2^+)=360 e^2\text{fm}^4$, whereas for the 4p-4h one we get $E(2^+)=0.17$ MeV and $B(E2)(2_1^+ \rightarrow 0_2^+)=555 e^2\text{fm}^4$.

For the full diagonalizations we use a truncation

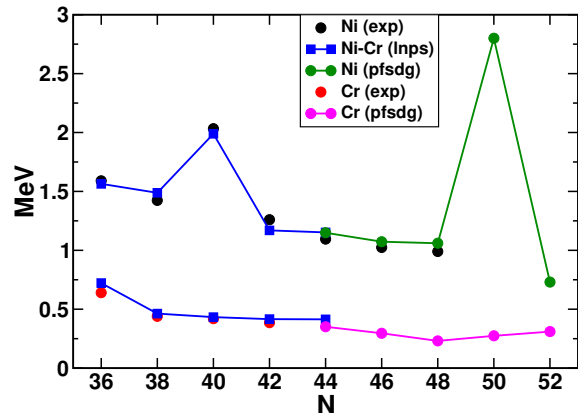


FIG. 6. (color online). 2^+ energy systematics in the Nickel and Chromium isotopic chains. Experimental data compared with calculations using the LNPS [?] and PFS DG-U interactions

scheme in terms of the sum of the number of neutron excitations across N=50 and proton excitations across Z=28 (t). Convergence is achieved typically for $t=8$. For ^{78}Ni we predict a doubly magic ground state at 65%, with a first 2^+ excited state at 2.88 MeV, that belongs to the (prolate) deformed band based in the intruder 0^+ which appears at 2.65 MeV of excitation energy, and a second 2^+ of 1p-1h nature at 3.15 MeV, with a large B(E2) to the ground state ($110 e^2\text{fm}^4$). In Figure 5 we include the yrast 4^+ which also belongs to the deformed band and a second 4^+ of particle hole nature. The $B(E2)(2_1^+ \rightarrow 0_2^+)$ goes up to $516 e^2\text{fm}^4$. Removing two protons, the ground state of ^{76}Fe turns out to be a very complicated mixture of np-nh configurations, including 20% of 0p-0h. The yrast 2^+ appears at 0.43 MeV and is rather of 2p-2h plus 4p-4h nature. This mismatch produces a certain quenching of the B(E2) relative to the spectroscopic quadrupole moment of the 2^+ as seen in Table I. Most interestingly, the first excited state is another 0^+ at 0.36 MeV which is also of very mixed nature, although now the 0p-0h components amount to 33%. Thus, the doublet of 0^+ states in ^{76}Fe is a consequence of the rapid transition from the doubly magic ground state of ^{78}Ni to the fully rotational case of ^{74}Cr , where the collective behaviour is fully established as the type of configurations which made the deformed excited band of ^{78}Ni become yrast, with a 2^+ at 0.27 MeV and $E(4^+)/E(2^+)=3$ (see Figure 5). Collectivity persists to a lesser extent in ^{72}Ti , whose 2^+ is at 0.41 MeV. There is no experimental information for these nuclei yet. Table I shows the calculated B(E2) values and spectroscopic quadrupole moments, which correspond, in the well deformed case of ^{74}Cr , to $\beta_{mass} \sim 0.3$

and $\beta_{charge} \sim 0.33$, in very nice agreement with the results of the PHF-PES. Finally, we gather in Figure 6 the evolution of the 2^+ excitation energies for the Nickel and Chromium chains. The present calculations are complemented towards $N=40$ with the results obtained using the LNPS interaction and valence space [14]. It is seen that the magic peaks at $N=40$ and $N=50$ in the Nickels disappear completely in the Chromiums; the fingerprint of the onset of deformation and of the entrance in the IoI's. The agreement of the SM-CI description with experiment may soon extend to full chains of isotopes from the proton to the neutron drip lines, for instance from ^{48}Ni and ^{44}Cr ($N=20$) in the pf -shell with the KB3G interaction, to ^{80}Ni and ^{76}Cr ($N=52$) using PFSGDG-U.

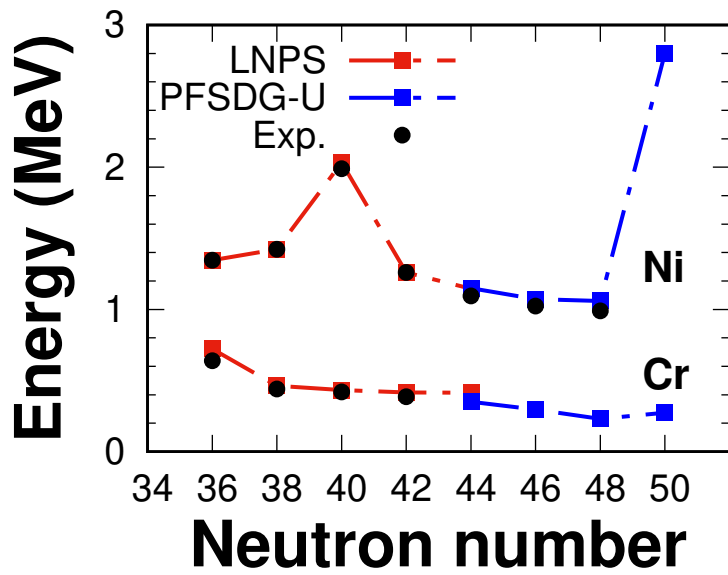
In conclusion, it looks as if Nature likes to replicate the $N=40$ physics at $N=50$. Shape coexistence in doubly magic ^{78}Ni turns out to be the portal to a new IoI at $N=50$ which merges with the well established one at $N=40$ for the isotopes with $Z \leq 26$. With this new addition, the archipelago of IoI's in the neutron rich shores of the nuclear chart counts now five members: $N=8, 20, 28, 40$, and 50 .

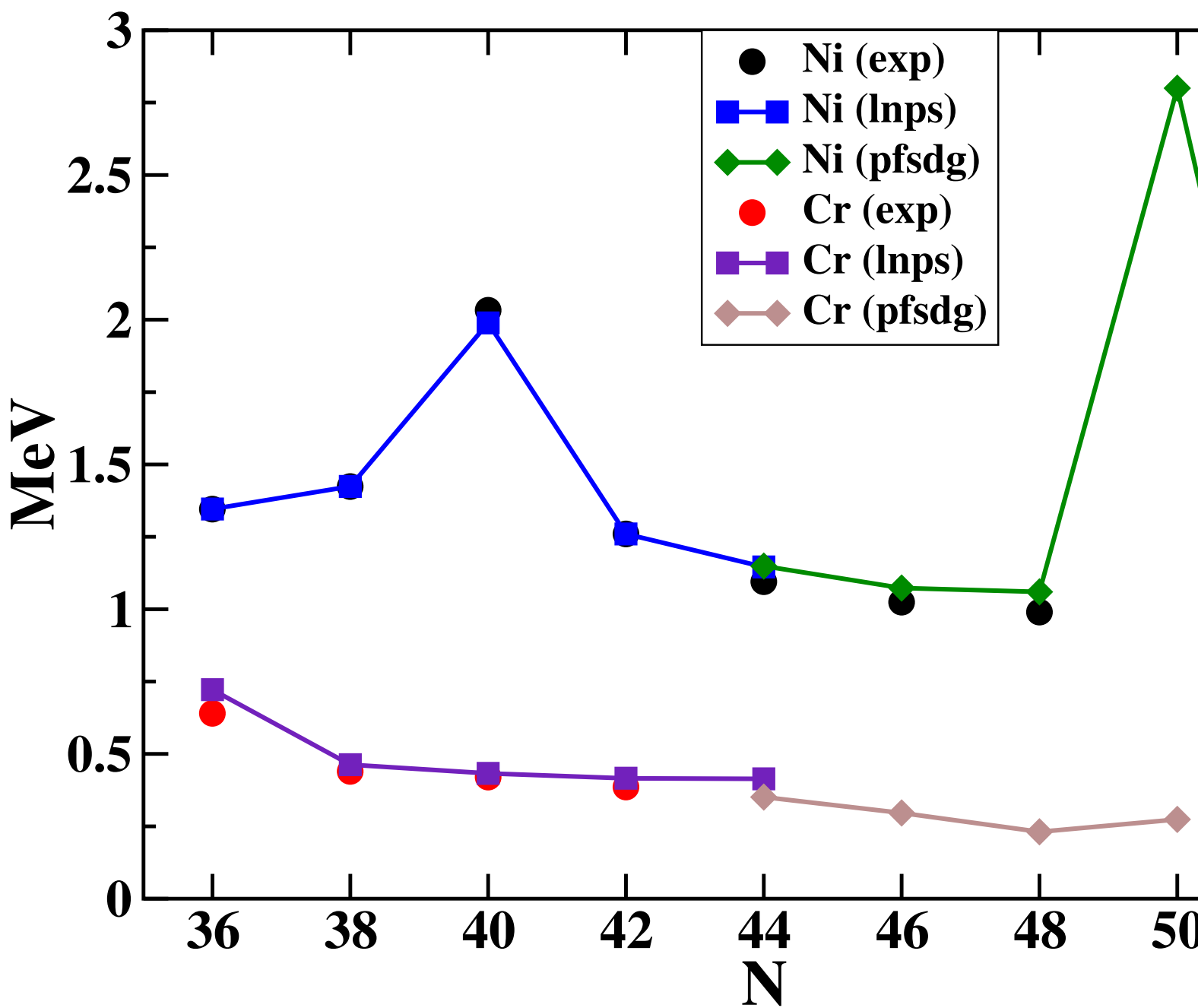
Note. A paper describing the heaviest Nickel isotopes with "ab initio" methods was posted in the arXiv [26] a few days ago. Both calculations agree in many aspects, the main difference being that their's does not produce the intruder, deformed, np-nh excited band, coexisting with the doubly magic states of ^{78}Ni .

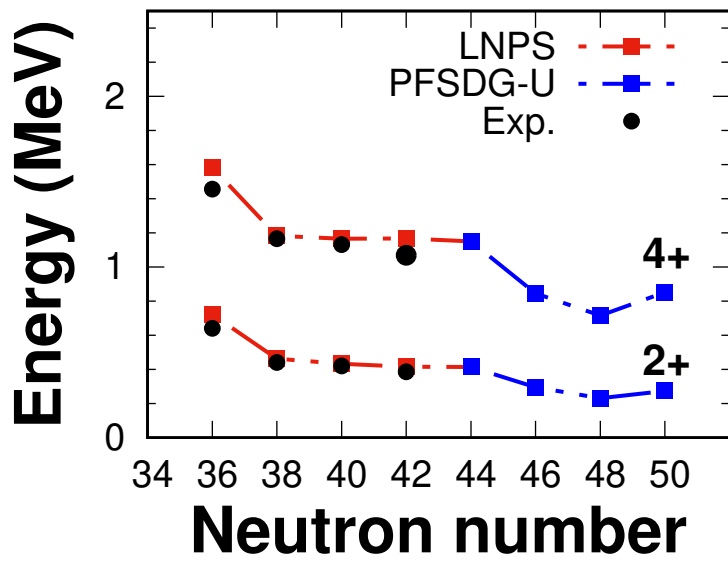
Acknowledgments. This work is partly supported by MINECO (Spain) grant FPA2014-57196 and Programme "Centros de Excelencia Severo Ochoa" SEV-2012-0249, and by an USIAS Fellowship of the Université de Strasbourg.

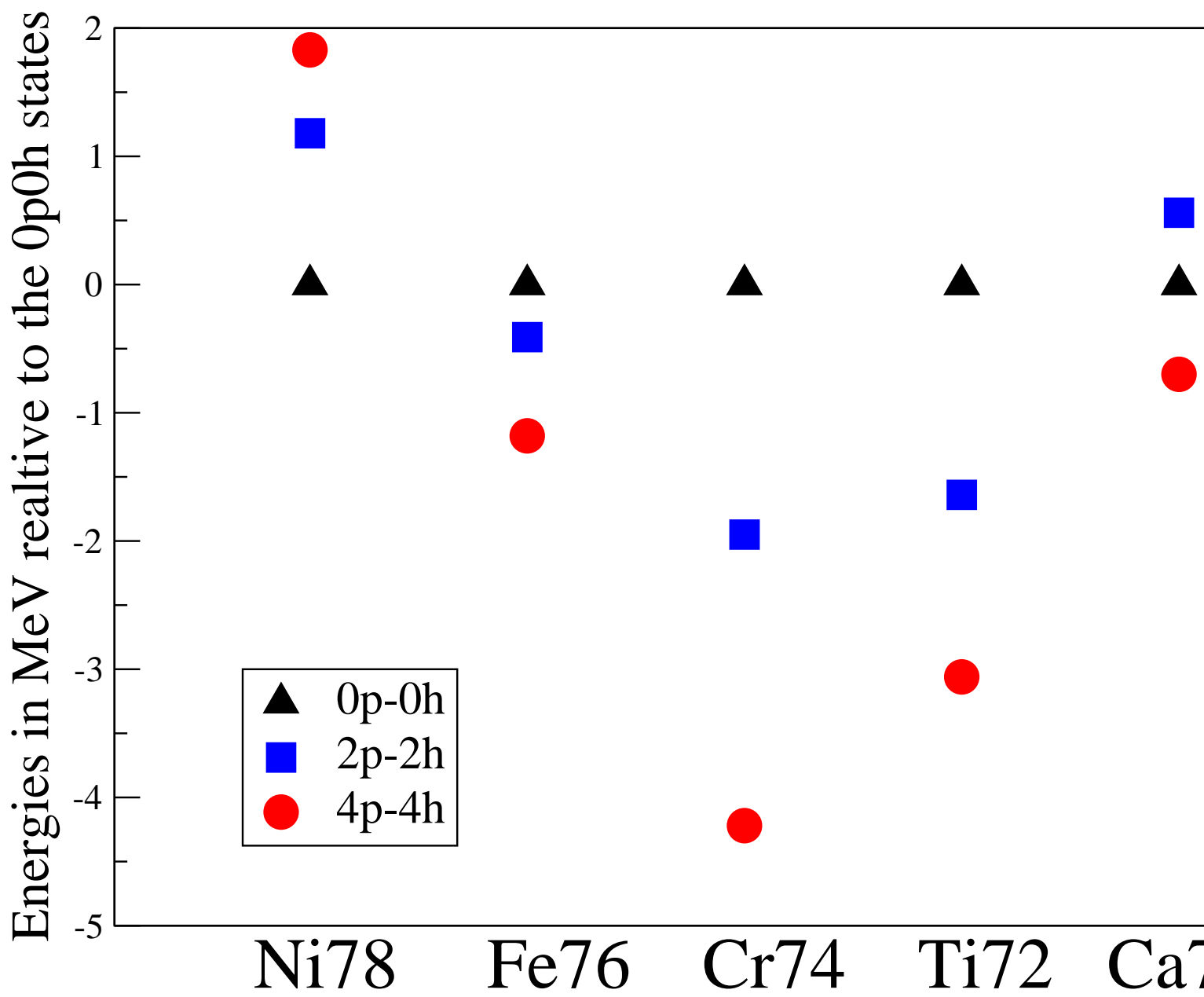
REFERENCES

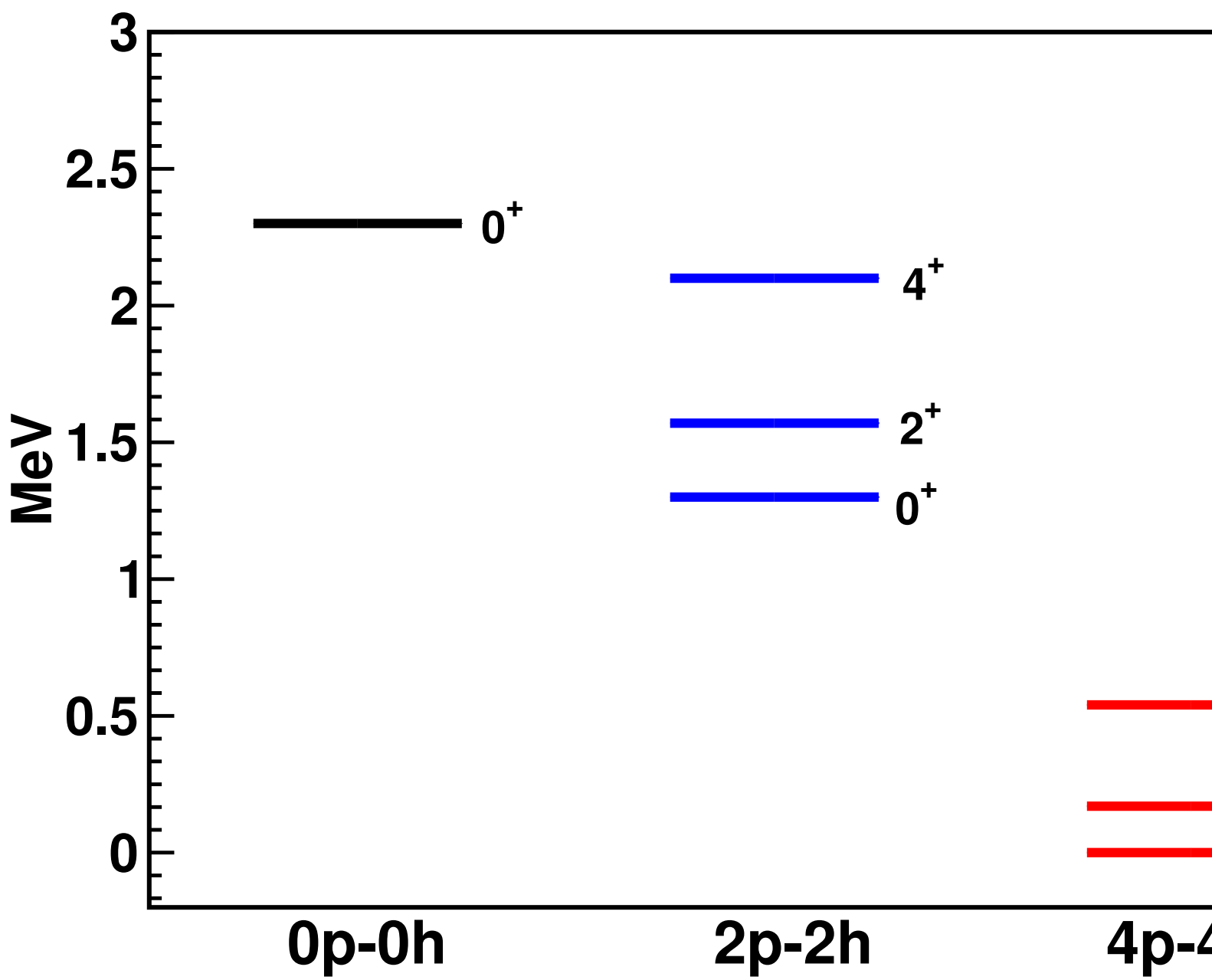
-
- [1] R. N. Wolf *et al.*, Phys. Rev. Lett. **110**, 041101 (2013).
 - [2] T. Otsuka *et al.*, Phys. Rev. Lett. **95**, 232502 (2013).
 - [3] T. Otsuka *et al.*, Phys. Rev. Lett. **104**, 012501 (2010).
 - [4] O. Sorlin *et al.*, Phys. Rev. Lett. **88**, 092501 (2002).
 - [5] M. Hannawald *et al.* Phys. Rev. Lett. **82**, 1391 (1999).
 - [6] W. Rother *et al.*, Phys. Rev. Lett. **106** 022502 (2011)
 - [7] J. Ljungvall *et al.*, Phys. Rev. C **81**, 061301 (2010).
 - [8] A. Gade *et al.*, Phys. Rev. C **81**, 051304 (2010).
 - [9] A. Dijon, *et al.* Phys. Rev. C **85** 031301 (2012).
 - [10] F. Recchia, *et al.* Phys. Rev. C **88** 041302(R) (2013).
 - [11] S. Suchyta, *et al.* Phys. Rev. C **89** 021301(R) (2014).
 - [12] T. Baugher, *et al.* Phys. Rev. C **86** 011305(R) (2014).
 - [13] H. L. Crawford, *et al.* Phys. Rev. Lett. **110** 242701 (2013).
 - [14] S. M. Lenzi, F. Nowacki, A. Poves, and K. Sieja, Phys. Rev. C **82** 054301 (2010).
 - [15] Y. Tsunoda, *et al.* Phys. Rev. C **89** 03133(R) (2014).
 - [16] P. Doornenbal, *et al.*, Phys. Rev. Lett. **111** 212502 (2013).
 - [17] E. Caurier, F. Nowacki, and A. Poves, Phys. Rev. C **90** 014302 (2014).
 - [18] C. Santamaria, *et al.*, Phys. Rev. Lett. **115** 192501 (2015).
 - [19] K. Sieja, and F. Nowacki, Phys. Rev. C **85** 051301 (2012).
 - [20] A. P. Zuker, A. Poves, F. Nowacki, and S. M. Lenzi, Phys. Rev. C **92** 024320 (2015).
 - [21] C. B. Hinke, *et al.*, Nature **486** 341 (2012).
 - [22] A. Arima, M. Harvey, and K. Shimizu, Phys. Lett. B **30** 517 (1969).
 - [23] K. Hecht, and A. Adler, Nucl. Phys. A **137** 129 (1969).
 - [24] R. Machleidt, Phys. Rev. C **63** 024001 (2001).
 - [25] M. Hjorth-Jensen, T. T. S. Kuo, and E. Osnes, Physics Reports **261** 126 (1995).
 - [26] G. Hagen, G. R. Jansen, and T. Papenbrock, arXiv:1605:01477.











(-) Quadrupole energy in Quasi+Pseudo SU3

